ARTICLE

Existence of Bound-Rubber in Magnetorheological Elastomers and Its Influence on Material Properties

Xian-zhou Zhang[a], Xing-long Gong[a]*, Pei-qiang Zhang[a], Wei-hua Li[b]

a. CAS Key Laboratory of Mechanical Behavior and Design of Materials, Department of Mechanics and Mechanical Engineering, University of Science and Technology of China, Hefei 230027, China; b. School of Mechanical, Materials and Mechatronic Engineering, University of Wollongong, Wollongong, NSW 2522, Australia

(Dated: Received on July 7, 2006; Accepted on November 3, 2006)

In efforts to develop a new fabrication method for improvement of the MREs' performance, the bound-rubber phenomenon was observed in MREs. Further experiments indicate the existance of bound-rubber and it influences the MRE performance as well as the particle size. Both theoretical analysis and experimental results indicated that MRE performance can be improved by enhancing the ratio of particle radius to bound-rubber thickness.

Key words: Magnetorheological elastomers, Bound-Rubber, Storage modulus

I. INTRODUCTION

Magnetorheological (MR) materials are a kind of intelligent material whose performance can be controlled by an applied magnetic field. Since the MR effect was discovered by Rabinow in 1948 [1], MR materials have become a large family with MR fluids, MR foams, MR elastomers (MREs) etc. [2]. Because of their quick response, good reversibility and controllable performance, MR materials have been widely used in various fields such as vehicle construction, building, and vibration control [1-7]. MREs are composed of micrometer size magnetizable particles and an elastomer matrix. The particles and liquid matrix material are mixed together before curing. Then the mixture is cured in the presence of a magnetic field. Some special structures, such as chains or columns of particles, remain in the matrix. When an MRE is exposed to an external magnetic field, its storage modulus changes with the intensity of the applied field. The maximum modulus increase of MREs has been reported to be nearly 0.6 MPa (40% of initial modulus) when iron volume concentration is 30% [8]. MREs combine the advantages of MR fluids and elastomers, overcoming the shortcomings of MR fluids, such as sedimentation and instability [9-12].

MREs can be used in many applications that require variable stiffness components, such as adaptive tuned vibration absorbers (TVAs), stiffness tunable mounts and suspensions, and variable impedance surfaces [2,8,9]. The Ford Motor Company has patented an automotive bushing employing MREs [13,14]. The stiffness of the bushing was adjusted to reduce suspension deflection and to improve passenger comfort. Although there are currently few reports on applications of MREs, it is still a promising material that can be used in many applications with its controllable stiffness and other unique characteristics [2].

Currently conventional MREs do not have large enough MR effects, which has limited their wide industrial application. Therefore, it is crucial to investigate new methods to improve MRE performance. During our efforts to develop new fabrication methods, we found the bound-rubber phenomenon existing in MREs. This paper presents the effects of the bound-rubber on the MRE performance.

II. EXPERIMENTAL OBSERVATION OF THE BOUND-RUBBER

Many kinds of MRE samples were prepared in order to study methods to improve the MR effect of MREs. To prepare the MRE samples, RTV silicon rubber and silicone oil were chosen as the matrix. Three types of carbonyl iron particles were used. Their average diameters were 3, 5 and 60 μm. Microscopic analysis of the particles revealed that the iron particles product consisted of a range of particle sizes clustered about a mean particle diameter of 3, 5 and 60 microns with a standard deviation of 1.6, 2.4 and 21 microns, respectively. After carbonyl iron particles had been immersed in silicone oil, they were mixed with RTV silicone rubber. Then the mixture was put into a vacuum case to remove the air bubbles inside it. After curing for about 24 h at room temperature with magnetic flux density about 1 Tesla, the MREs were prepared. The volume fractions of particles in our samples were all 40%.

To observe the MRE microstructure, a slice of each MRE was placed into an environmental scanning elec-

*Author to whom correspondence should be addressed. E-mail: gongxl@ustc.edu.cn

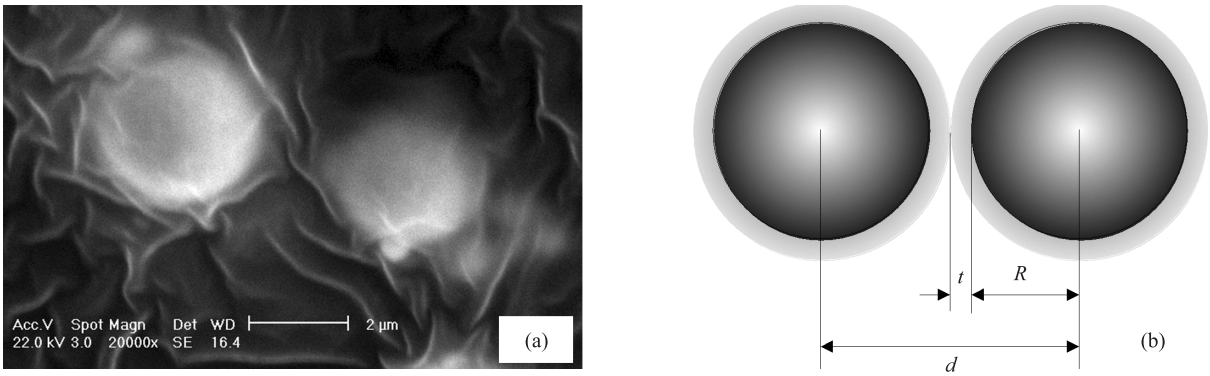

FIG. 1 Bound-rubber around iron particles: (a) SEM photo of MREs (with 3 μm particles), (b) Sketch map of particles with bound-rubber.

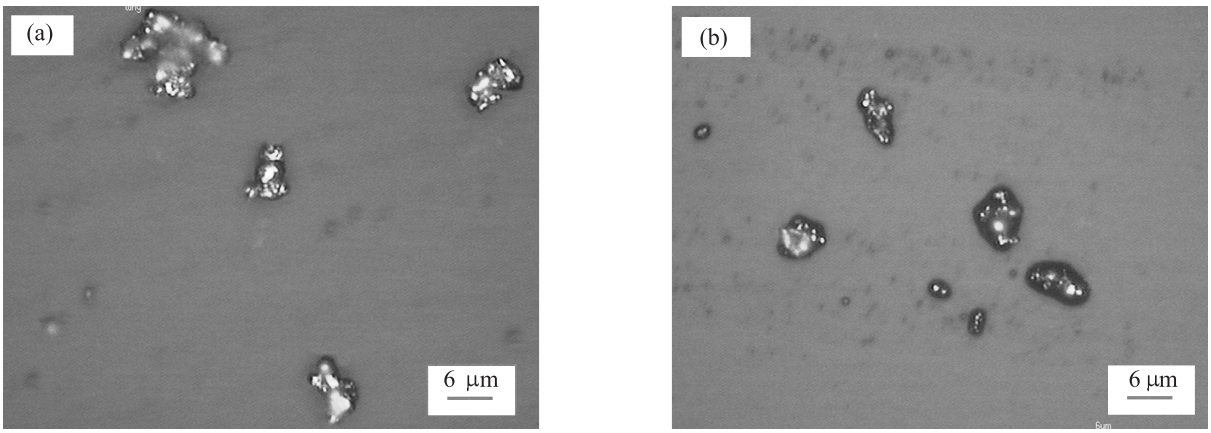

FIG. 2 Micrographs of particles. (a) Photo of pure carbonyl iron particles, (b) Photo of particles with bound-rubber.

tron microscope (Model: XT30 ESEM-TMP, made by Philips of Holland). Figure 1(a) shows a typical microstructure of the prepared MREs. It is observed that a thin layer covers the surface of the iron particles. Based on the SEM result, a simple bound-rubber model is proposed, as shown in Fig.1(b).

The micrographs of pure carbonyl iron particles observed by metallographic microscope (Type: CMM-55E, Shanghai Changfang Optical Instrument Co., Ltd. China) are shown in Fig.2(a), where the surface of the particles is clean. In order to observe the surface of particles in MREs, a sample was immersed in boiling methylbenzene till the solvent dissolved the matrix. After washing the residual, the particles with the layer were obtained. Figure 2(b) shows the micrographs of these particles. Bound-rubber can be observed clearly on the surface of these particles. Their thickness was about 0.7 μm.

The differential thermal analysis (DTA) and thermogravimetry analysis (TGA) method were used to characterize the layer properties [15,16] using type model TA-50, made by SHIMADZU Inc. of Japan. The experimental conditions were as follows: atmosphere: air; cell: alumina; temperature rate: 10.00 °C/min; hold temperature: 800 °C. The carbonyl iron powder, rubber matrix and the MREs sample were tested respectively. Their DTA and TGA curves are shown in Fig.3 (a) and (b), respectively. The exothermic peak I in Fig.3(a) indicates that the iron powder oxidizes in oxidative environment about 460 °C. The same place in Fig.3(b) shows the weight of the sample becomes larger because the sample changes from iron to ferric oxide. This confirms the oxidative phenomenon. The exothermic peak II in Fig.3(a) shows that the rubber matrix combusts in oxidative environment at about 552 °C. The same place in Fig.3(b) indicates that the weight of the sample becomes smaller because some elements in the sample, such as carbon, hydrogen and oxygen reacted and became gas. This confirms the combustion phenomenon.

About the curves of the MREs, as shown in Fig.3(a), the exothermic peak A has the same meaning as peak II. The reaction point of silicone rubber moves from 552 °C to 506 °C because of the iron's catalysis. The same place in Fig.3(b) shows that the weight of the sample becomes less there. But the exothermic peak B is not in the same place as the iron powder's oxidization because the same place in Fig.3(b) still has the weight

ISSN 1003-7713/DOI:10.1360/cjcp2007.20(2).173.7

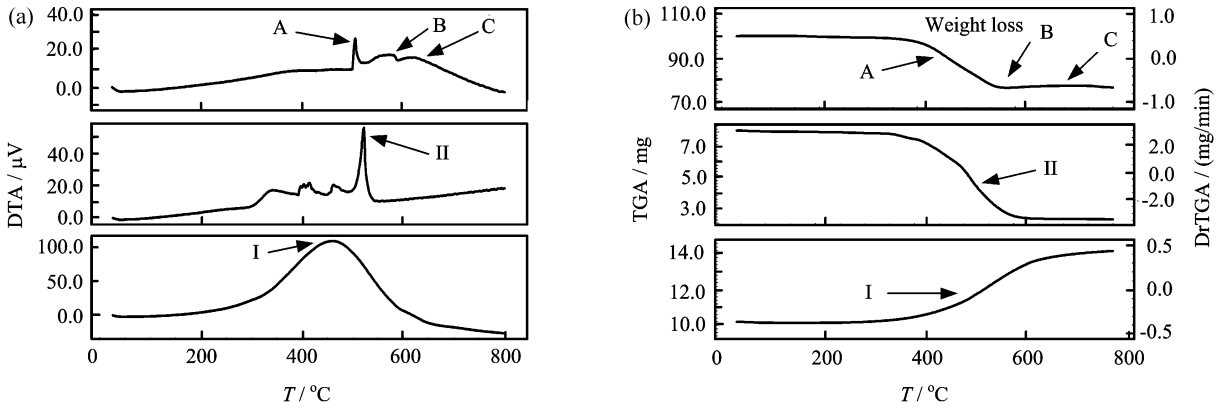

FIG. 3 DTA (a) and TGA (b) curves of MREs, silicone rubber and carbonyl iron powder.

loss trend. This is caused by the combustion of the layer that covered the particle. That layer has different behavior from the matrix and its reaction point is about 570 °C. The oxidization of iron powder is restrained by the layer wrapped around it and it does not react until the layer is burned out, so the reaction point of iron powder changes from 460 °C (the exothermic peak I) to 620 °C (the exothermic peak C). The same place in Fig.3(b) shows that the weight of the sample becomes larger then. By these experiments, it can be found that this kind of layer has different properties from particle or rubber matrix because it has its special exothermic peak B. It marks the transition layer between particle and rubber matrix. We call the layer bound-rubber.

As a matter of fact, the bound-rubber is in existence in tire rubbers. It is the gel on the surface of carbon black in tire rubber. The bound-rubber fraction of an uncured compound is the amount of rubber that is not extracted when it is exposed to a good solvent. In fact, the bound-rubber is the rubber that is trapped by the particles after mixing. It is the rubber between the interface of the carbon black and the rubber layer. The rubber chains are attracted either physically or chemically to form a rubber shell on the surface of the carbon black particle. The rubber that is attached closest to the carbon black molecule is much stiffer than the rubber molecules that are further away. Nuclear magnetic resonance imaging (NMR) studies have confirmed the existence of a rubber shell around filler particles [17-20]. The tire rubber with the higher volume fraction bound-rubber has the better effect of reinforcement. Similar to carbon black gel complex, the bound-rubber in MREs is the rubber between the interface of the iron particles and the rubber matrix.

III. BOUND-RUBBER'S INFLUENCE ON MRE MECHANICAL BEHAVIOR

To study the bound-rubber's influence on the MRE performance, the zero-field modulus and modulus increase due to an applied magnetic field were analyzed. Theoretical results were also compared with experimental results.

A. Influence on zero-field modulus of MREs

By using the Guth-Gold equation, Davis analyzed the relationship between the zero-field modulus of MREs and the volume fraction of iron particles [20]:

$$G = G_0(1 + 2.5\phi + 14.1\phi^2) \tag{1}$$

where G is the shear modulus of MREs without a magnetic field, G_0 is the shear modulus of the pure matrix, and ϕ is the volume fraction of particles. In this equation, the influence of the bound-rubber and the interactions among particles are not taken into account.

In fact, because of the presence of bound-rubber, a part of the rubber cannot flow or transform as freely as the rubber in matrix. To analyze clearly, the interface-effect of bound-rubber is omitted, only the volume effect of bound-rubber is considered. Some volume fraction of the bound-rubber ought to be calculated as the volume fraction of particles, i.e. the ϕ in Eq.(1) should be modified according to the effective volume fraction.

According to the simple bound-rubber model shown in Fig.1(b), w is defined as the power coefficient to convert the thickness of bound-rubber to effective thickness of particle surface, the effective volume of a particle is $\frac{4}{3}\pi(R + wt)^3$. Different matrixes have different w, which can be obtained by experiments. In the equation t is the bound-rubber thickness and R is the iron particle radius.

The zero-field shear modulus G' of MREs can be written as:

$$G' = G_0\left[1 + 2.5\left(\frac{R + wt}{R}\right)^3\phi + 14.1\left(\frac{R + wt}{R}\right)^6\phi^2\right] \tag{2}$$

The G' calculated by this equation takes the bound-rubber thickness and particle radius into account.

ISSN 1003-7713/DOI:10.1360/cjcp2007.20(2).173.7

According to Eq.(2), the shear modulus increases with increasing ϕ. Meanwhile, the thickness of the bound-rubber and the radius of the iron particle also influence the zero-field modulus of MREs: the less the particle's radius, the larger the MREs's modulus, because with the same volume, small particles have larger surface area than large ones, and they have more volume fraction bound-rubber. Eq.(2) indicates the bound-rubber's influence on the zero-field shear modulus of MREs. Fixing 30% volume fraction of particles, the calculated result is shown in Fig.4. It gives the relationship between G'/G_0 and R/wt. When $R/wt\to 0$, it means the particles are very fine and they have much bound-rubber. This kind of MRE has high zero-field shear modulus. If the ratio of R/wt increases, it means that the particle's size becomes larger or the bound-rubber's thickness becomes less. As a result, the zero-field shear modulus of MREs becomes less and less. When $R/wt\to\infty$, it means that there is no bound-rubber and the value of the modulus is close to the result obtained by Eq.(1). If the bound-rubber's thickness has the same value, along with the increase of particles' radius, the shear modulus has a descending trend. This shows that the larger particles reduce the material's zero-field modulus. When the particle radius is large enough (about $100wt$), this effect can be neglected.

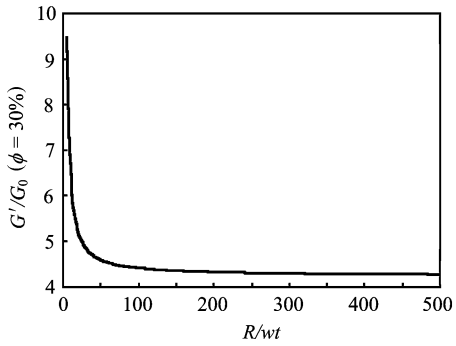

FIG. 4 Increase factor of shear modulus without magnetic field *vs.* R/wt.

B. Influence on the MR effect of MREs

The current theoretical research considers that the ratio of particle radius to the distance between the particles along the magnetic field's direction greatly influences the MR effect [21,22]. In the following paragraphs, the bound-rubber's influence on MR effect is discussed based on these research results.

As shown in Fig.1(b), the particles cannot contact each other and the distance between their surfaces is at least $2t$. This is because a bound-rubber layer with low permeability is absorbed by the particles. Therefore the least distance between two particle centers is $2(R+t)$.

For ease of explanation, the MRE modulus increase is discussed only when the particles are completely saturated. For consideration of the dynamic properties of MR material before saturation [21,22]. In saturation, the increase in shear modulus due to magnetic field is the maximum. The particles cannot be looked on as a point located at the center of the particle when the distance between the particles is very small. Here it is assumed that the particle is composed of a series of thin layers along the chain, as shown in Fig.5. The magnetic energy for two neighboring particles is modified as [21]:

$$E=\int_{-R}^{R}\int_{-R}^{R}\frac{\cos^3\theta-3\cos^5\theta}{4\pi\mu_0(d+z_2+z_1)}\mathrm{d}m_1\mathrm{d}m_2 \tag{3}$$

$$\begin{aligned}\mathrm{d}m_1&=\pi\mu_0 M_s(R^2-{z_1}^2)dz_1\\ \mathrm{d}m_2&=\pi\mu_0 M_s(R^2-{z_2}^2)dz_2\end{aligned} \tag{4}$$

where μ_0 is the vacuum permeability, M_s is the saturation magnetization of particles and d=2(R+t).

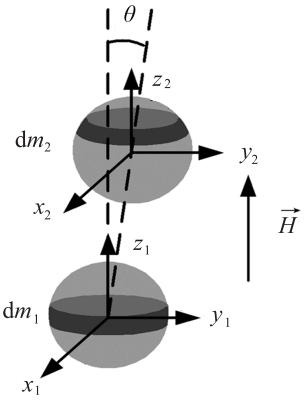

FIG. 5 The model for magnetic saturation.

The energy per unit volume is:

$$E_d=\frac{3\phi}{4\pi R^3}E \tag{5}$$

Now we calculate the shear modulus increase due to the magnetic field. For small deformation, $\theta\to 0$, according to the relationship between the energy and the shear strain, the modulus increase due to applied magnetic field can be expressed as:

$$\begin{aligned}\Delta G_{\max} &= 3\zeta\phi {M_s}^2\mu_0\Big[2\ln(k+1)-2\ln(2k+1)\\ &\quad+2+\frac{2\ln(2k+1)-4\ln(k+1)}{k^3}\\ &\quad+\frac{6\ln(2k+1)-12\ln(k+1)}{k^2}\\ &\quad+\frac{2-6\ln(k+1)+3\ln(2k+1)}{k}\Big]\end{aligned} \tag{6}$$

where $\zeta\approx 1.202$ denotes the influence of all the particles in a chain along the magnetic field direction and k=R/t.

ISSN 1003-7713/DOI:10.1360/cjcp2007.20(2).173.7

Fixing 30% volume fraction of particles, the relationship between ΔG and R/t is given in Fig.6. As shown in Fig.6, when $R/t \to 0$, the particles are very fine and there are thick bound-rubber layers covering particles. This kind of MRE has almost no MR effect. The MR effect is very low when particle radius and bound-rubber thickness are of the same magnitude. If the thickness of bound-rubber is a fixed value, the MR effect will enhance quickly along with the increase of particle radius. When $R/t \to \infty$, it means there is little bound-rubber and the particles can touch each other. This kind of MRE has maximum MR effect. And when the particle radius is large enough (about $100t$), this effect is no longer obvious. This analysis indicates that the MREs with larger ratio of R/t has larger MR effect.

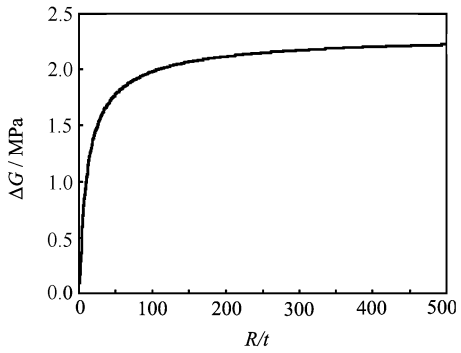

FIG. 6 The maximum increase of modulus *vs.* R/t. ($\mu_0 M_s \approx 2.1$ T, ϕ=30%).

Because of the complexity of the analysis in undersaturated condition, only the saturated condition is discussed. The MRE performance in different magnetic flux density will be analyzed using the experiment result that follow.

C. Experiment results

The mechanical performance of MRE samples was measured using the system developed by our group, illustrated in Fig.7. The magnetic intensity was controlled by the electrical current intensity in the electromagnetism system (Peking EXCEEDLAN Inc., China) and measured by a Tesla gauge (model: CT3-A, made by Shanghai No.4 Electric Meter Factory, China). The MRE sample, with its upper and lower surfaces adhered to two copper slabs, was inserted into the gap of the magnetic pole. The basic slab was forced to vibrate by an exciter (JZQ-2), which was driven by a random signal source from a power amplifier whose signal was provided by a HP35665A Dynamic Signal Analyzer (HEWLETT PACKARD Inc. of USA). The power amplifier (GF20-1) is made by BAOYING BAOFEI vibration instrument factory in China). The vibrations were monitored by piezoelectric acceleration transducers (CA-YD-103). The signals from the transducers were input into charge amplifiers (YE5858A, SINOCERA PIEZOTRONICS INC. China). Then they were sent to the HP35665A Dynamic Signal Analyzer for processing and analysis.

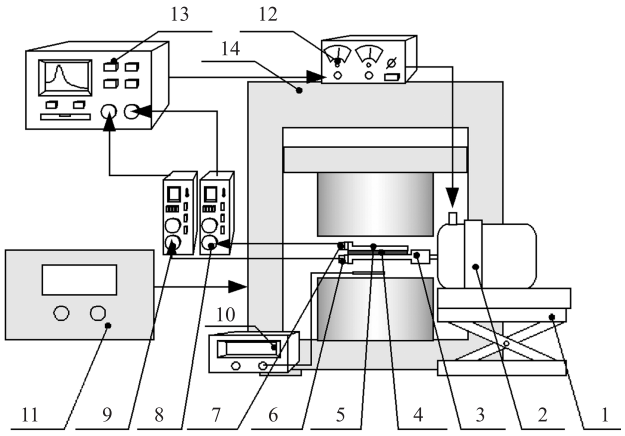

FIG. 7 MREs' performance testing setup. 1. Adjustable base; 2. Exciter; 3. Copper slab 1; 4. Sample; 5. Copper slab 2; 6. Acceleration transducer 1; 7. Acceleration transducer 2; 8. Charge amplifier1; 9. Charge amplifier 2; 10. Tesla gauge; 11. DC power Supply; 12. Power amplifier (for exciter); 13. HP35665A dynamic signal analyzer; 14. Electromagnet.

By analyzing the vibrating signals, the mechanical parameters (such as storage modulus and loss factor) of MREs can be calculated. The correlated coefficients of the two transducers' signals can also be displaced on the analyzer. The minimum coefficient is about 0.97, so the reliability of the system is good enough. The detail of this system was introduced in our previous work [22].

The samples' performances were tested and Fig.8 illustrates the storage modulus (at 200 Hz) of MRE samples with different particles (versus magnetic flux density). As shown in Fig.8, the shear modulus of MREs increases with increasing magnetic flux density, and it is saturated in the high field region. The modulus saturation takes place after 800 mT. The zero-field shear

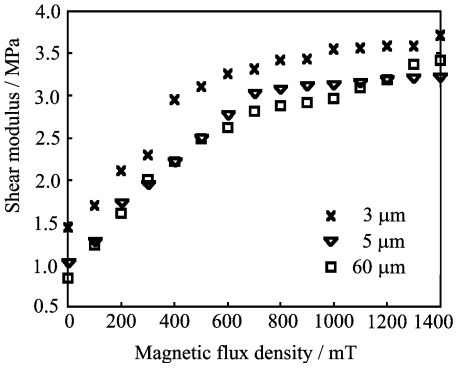

FIG. 8 Shear modulus of MRE samples (at 200 Hz) with different diameter particles *vs.* magnetic flux density.

ISSN 1003-7713/DOI:10.1360/cjcp2007.20(2).173.7

modulus of the MREs with 3, 5 and 60 μm particles are about 1.4, 1.0 and 0.8 MPa respectively. Their maximum modulus increases under magnetic flux density 1.4 Tesla are 2.3, 2.9 and 3.4 MPa respectively. Although the modulus increase due to applied magnetic field of the MREs with 3 μm particles is the least in all samples, its final shear modulus under magnetic flux density 1.4 Tesla is still higher than that of the MREs with 5 or 60 μm particles because it has the highest zero-field modulus.

Comparing the zero-field shear modulus of samples with different particles, it is found that the larger the iron particles are, the less the zero-field shear modulus is. The modulus difference between the MREs with 3 μm particles and the MREs with 5 μm is larger than the modulus difference between the MREs with 5 μm particles and the MREs with 60 μm. Referring to Eq.(2) and Fig.4, it is found that this result agrees well with the theoretical analysis of the bound-rubber's influence on MRE zero-field modulus. Comparing the maximum absolute increase of modulus due to magnetic field, it can be found that the MREs with larger particles have larger MR effect. Also the difference between the MREs with 5 μm particles and the MREs with 60 μm particles is not as much as that between the MREs with 3 μm particles and the MREs with 5 μm particles. Referring to Eq.(7) and Fig.6, it is found that this result is also in accord with the theoretical analysis of the bound-rubber's influence on MRE shear modulus increase due to applied magnetic field.

Furthermore, the experimental results in reference [23] also proved the rationality of this theory. In reference [23], by using a "clamped-free" vibrating sandwich beam, the dynamic characteristics (storage modulus and loss factor) of a number of MREs have been measured. The influence of such parameters as the type of carrying matrix, the size of ferromagnetic-filler particles, and the intensity of action by the external magnetic field has been evaluated. Three size of filler particles (3.5, 13, and 23 μm, respectively) were used to fabricate MREs, and the dynamic characteristics of the sandwich (modulus of the damping layer of the MREs and the entire sandwich) in different magnetic field intensity (0-600 mT) were tested. It is found that the larger the particles of ferromagnetic filler are, the larger the modulus increase is. The situation is the reverse in the absence of the field: the MREs filled with larger particles are more plastic. Comparing the experiment results in reference [23] with our experiment results, it is found that they show the same trends.

These experiments are in accord with the theoretic analysis of bound-rubber in MREs. If the thickness of the bound-rubber in MREs is constant, the MREs fabricated with larger particles have larger MR effect and less zero-field modulus. If the particles' radius is constant, the less the thickness of the bound-rubber around the particles is, the larger the MR effect is, and the less the zero-field modulus is. But the ratio of R/t can not be too large because the stretch strength and the hardness of elastomers will be reduced along with the increasing of this ratio [17,18]. This means that appropriate bound-rubber thickness and particle radius are key factors to improve the performance of MREs.

IV. CONCLUSION

The thickness of bound-rubber will influence the performance of MREs as well as the particles' radius. This phenomenon ought to be considered while fabricating and using MREs.

1. When the bound-rubber thickness and the particle radius have the same magnitude, the increase of particle radius lowers the zero-field modulus of MREs notably. This effect is no longer obvious when the particle radius is at least 100 times as large as wt.

2. The increase of particle radius will enhance the MR effect of MREs notably if the bound-rubber thickness and the particle radius are of the same magnitude. When the particles' radii are over 100 times as large as the bound-rubber thickness, this effect is no longer obvious.

3. It is well known that tire rubber with more volume fraction carbon black gel complex has the better mechanical performance. In order to improve the synthesizing performance of MREs, the particle radius must be chosen carefully in a certain bound-rubber thickness. The radius ought to be about 100 times as large as the bound-rubber thickness. By this method, the relative modulus increase of MREs due to applied magnetic field can be enhanced while not weakening the material's strength excessively.

4. Appropriate bound-rubber thickness can also improve the performance of MREs. To realize it, some method can be used, such as pretreating the particles' surface before mixture, quickening the speed of mixture, improving the temperature while mixing, using a rubber matrix with less molecular weight or compressing the mixture along the direction of magnetic field while the MRE is being vulcanized [21].

V. ACKNOWLEDGMENTS

This work was supported by the National Natural Science Foundation of China (No.10672154), Specialized Research Fund for the Doctoral Program of Higher Education of China (No.20050358010) and Scholarship Bai Ren Ji Hua funding of the Chinese Academy of Sciences.

[1] J. Rabinow, AIEE Transactions **67**, 1308 (1948).
[2] J. D. Carlson and M. R. Jolly, Mechatronics, **10**, 555 (2000).

ISSN 1003-7713/DOI:10.1360/cjcp2007.20(2).173.7

[3] W. H. Li, G. Z. Yao, G. Chen, S. H. Yeo and F. F. Yap, Smart Materials & Structures **9**, 95 (2000).
[4] W. H. Li, H. Du, G. Chen, S. H. Yeo and N. Q. Guo, Smart Materials & Structures **11**, 209 (2002).
[5] W. Q. Jiang, C. L. Zhu, Z. Y. Chen and P. Q. Zhang, Chin. J. Chem. Phys. **15**, 146 (2002).
[6] W. Q. Jiang, C. L. Zhu, Z. Y. Chen and P. Q. Zhang, Chin. J. Chem. Phys. **14**, 543 (2001).
[7] J. X. Wang and G. Meng, Chin. J. Chem. Phys. **14**, 548 (2001).
[8] M. R. Jolly, J. D. Carlson, B. C. Munzo and T. A. Bullions, J. Intelligent Material System and Structure **7**, 613 (1996).
[9] H. Dang, Y. S. Zhu, X. L. Gong and P. Q. Zhang, Chin. J. Chem. Phys. **18**, 971 (2005).
[10] Y. S. Zhu, X. L. Gong, H. Dang, X. Z. Zhang and P. Q. Zhang, Chin. J. Chem. Phys. **19**, 126 (2006).
[11] X. L. Gong, J. F. Li, X. Z. Zhang and P. Q. Zhang, J. Functional Materials **37**, 733 (2006).
[12] L. Chen, X. L. Gong, W. Q. Jiang and P. Q. Zhang, J. Functional Materials **37**, 703 (2006).
[13] J. R. Watson, US Patent. No.5609353 (1997).
[14] W. M. Stewart, J. M. Ginder, L. D. Elie, Nichols and E. Mark, US Patent. No.5816587 (1998).
[15] Z. D. Fang, D. J. Wang and C. Y. Zhang, Chin. J. Chem. Phys. **18**, 619 (2005).
[16] W. R. Zeng, S. F. Li and Y. J. Zhou, Chin. J. Chem. Phys. **16**, 317 (2006).
[17] Q. Z. Yang, *Modern Rubber Technology*, Beijing: China Petrochem Press, 194 (1997).
[18] L. Q. Zhang, Y. P. Wu, Y. Q. Wang, Y. Z. Wang, H. F. Zhang, D. S. Yu and J. Y. He, China Synthetic Rubber Industry **23**, 71 (2000).
[19] S. Wang, X. L. Lou, D. Z. Ma and Y. P. Huang, Chin. J. Chem. Phys. **17**, 652 (2004).
[20] L. C. Davis, J. Appl. Phys. **85**, 3348 (1999).
[21] X. Z. Zhang, X. L. Gong and P. Q. Zhang, J. Appl. Phys. **96**, 2359 (2004).
[22] X. L. Gong, X. Z. Zhang and P. Q. Zhang, Polymer Testing **24**, 669 (2005).
[23] S. A. Demchuk and V. A. Kuz'min, J. Eng. Phys. Thermophys. **75**, 396 (2002).

ISSN 1003-7713/DOI:10.1360/cjcp2007.20(2).173.7